International Conference on Computing in Civil and Building Engineering (ICCCBE)
25-28 August 2024, ÉTS, Montréal, Québec, Canada

Multi-agent-based swarm gas source localization using nano aerial robots

Jan Stührenberg[1], Felix S. Häusler[1], Patrick P. Neumann[2], Kosmas Dragos[1], and Kay Smarsly[1]

[1] Institute of Digital and Autonomous Construction, Hamburg University of Technology, Hamburg, Germany
[2] Bundesanstalt für Materialforschung und -prüfung (BAM), Berlin, Germany
jan.stuehrenberg@tuhh.de

Abstract

Gas source localization (GSL) is crucial for mitigating the impact of industrial accidents and natural disasters, for example finding leaks in oil and gas facilities or survivors in collapsed environments. Traditional GSL methods involving human intervention may be hazardous and time-consuming. Utilizing swarms of agile and cost-effective nano aerial robots holds the potential to enhance the safety and efficiency of GSL operations. This study draws inspiration from biological swarms, particularly colonies of social insects, to coordinate and optimize the performance of nano aerial robotic swarms. While most existing swarm GSL strategies assume gas concentration maxima to be in close proximity to actual gas sources, recent research has highlighted the importance of "bouts" as a more precise indicator of gas source proximity, considering the intermittency of gas distributions. In this paper, a swarm GSL strategy is introduced that incorporates bouts as indicators of source proximity, complemented by a bio-inspired pheromone communication system. Specifically, nano aerial robots are deployed as autonomous agents. Upon detecting bouts, the agents emit pheromone markers in an artificial environment, mimicking social insects. Using the concept of artificial potential fields, the agents either exploit the search space by following pheromone gradients or explore the search space. The proposed swarm GSL strategy is implemented and validated in a real-world experiment, conducted in an indoor environment with a single gas source. The experimental results demonstrate the capability of the swarm GSL strategy to perform effectively in indoor environments and that the intermittency of gas distributions is a better source proximity indicator than the mean concentration. It is concluded that this research may provide a methodological basis for improving gas source localization techniques and enhancing disaster response capabilities.

Keywords: Gas source localization, nano aerial robots, mobile robotic olfaction, bouts, swarm robotics.

1 Introduction

Gases may pose hazards to organisms, due to the toxicity or flammability. Therefore, gas source localization (GSL) becomes imperative to avoid danger and is the first step towards closing gas leaks in a range of industrial, environmental, and humanitarian applications. Robots may be used to perform GSL, which is exceptionally useful in environments that are dangerous and/or difficult to access. Employing multiple robots may enhance search efficiency, but requires dependable coordination. Taking inspiration from biological swarms, such as communities of social insects, is a widely explored avenue for achieving robust coordination among numerous yet simple agents. In the realm of mobile robot olfaction (MRO), much research has been inspired by swarm behavior approaches that interpret GSL as a concentration optimization problem, assuming the gas concentration maximum closely approximates a source location [1]. Given this premise, prevailing swarm intelligence algorithms may be applied to address GSL.

Particle swarm optimization (PSO) and ant colony optimization (ACO) are among the most widely used algorithms for GSL performed by multiple robots, as shown in a recent review [2]. The review included 46 studies, of which 30 studies used PSO and 6 studies used ACO. However, PSO and ACO simplify the tangible and dynamic elements of the environments for computational optimization by assuming no physical interaction between the agents. Deriving direct inspiration from biological swarms may yield algorithms that are simpler yet more effective, given that biological swarms function under comparable conditions to robotic swarms. In addition, numerous investigations have illustrated that the concentration maximum may not always serve as an effective indicator of source proximity in complex environments. Alternatively, the intermittency of gas plumes, assessed by so-called "bouts", may offer a more viable option [3].

In an attempt to counteract the disadvantages of PSO and ACO, this study introduces a swarm GSL strategy using bouts as proximity indicators, coupled with pheromone communication inspired by biological swarms (Section 2). Whenever agents detect bouts, the agents emit artificial pheromones at the respective position into an artificial environment. Based on the artificial environment, virtual forces are computed for navigation and collision avoidance with the artificial potential field (APF) concept. To maintain a balance between exploitation and exploration, agents

switch between (i) following pheromone gradients and (ii) investigating uncovered areas in the search space. Source estimation is determined by the highest concentration of pheromones in the artificial environment. The swarm GSL strategy is implemented and validated in simulations and real-world experiments (Section 3). The paper closes with conclusions and future work (Section 4).

2 Bout-based swarm GSL strategy

The swarm GSL strategy presented in this study comprises two integral components. In Section 2.1, the artificial (i.e., computational) environment is described, which is responsible for coordinating the swarm. Section 2.2 covers the agents, which are tasked with collecting measurements and emitting pheromones into the artificial environment upon detecting bouts. Furthermore, the interactions of the agents and the artificial environment are described.

2.1 Artificial environment

The artificial environment serves the purpose of facilitating efficient collaboration among the agents and is implemented through the APF concept [5]. Two different types of requests can be sent by the agents to the artificial environment, (i) the deposition of artificial pheromones in the artificial pheromone map (APM), which is part of the artificial environment, and (ii) the attractive and repulsive forces applying at the current position of the agents. The attractive forces are calculated from the APM and the repulsive forces are calculated in the so called "anti-collision component" based on the distances of the agents to walls and other agents.

Artificial pheromone map. The APM mimics the role of the environment in biological pheromone communication. The purpose of the environment in pheromone communication is characterized by two facets, (i) an arbitrary number of signals is integrated into a spatial function, and (ii) the spatial function is diffused over time. The first facet allows an arbitrary number of simple agents to cooperate without mutual awareness, while the second facet introduces a probabilistic functionality, as the effect of individually deposited pheromones diminishes over time unless the pheromones are consistently reinforced. The representation of the APM involves a discrete map covering the search space, where agents deposit pheromone markers of predetermined size and intensity at their respective locations. Following the deposition of a new pheromone marker, a diffusion kernel is applied to the APM. The event-based diffusion of pheromone markers, compared to the natural continuous diffusion in a real environment, avoids the loss of information when no new pheromone markers are deposited for a while. Still, the event-based diffusion gives newer entries more weight than earlier ones. For computing the attractive force, a copy of the APM is again smoothed with a diffusing kernel and then transformed into an APF. In this process, the kernel size governs the range of influence exerted by the pheromone markers. Subsequently, the gradient of the APF is calculated, resulting in a force field, and vortexed based on the following expression:

$$F_{vortex,x} = F_x + F_y \cdot \gamma, \tag{1a}$$

$$F_{vortex,y} = F_y - F_x \cdot \gamma, \tag{1b}$$

where $F_{vortex,x/y}$ represents the resultant vortexed force, $F_{x/y}$ denotes the initial force in the *x/y* direction, and γ is a factor that determines spin direction and vorticity. The vortexation results in agents not being attracted in a straight line to the current local pheromone maximum, but instead circling around the "promising" area. The circling behavior avoids repeated visits and thus the reinforcement of local optima. Finally, the vortexed force field is normalized to the range [0, 1]. The normalization ensures that the force is in a predefined range, which ensures that within a certain minimum distance from other agents and obstacles, the repulsive force always dominates to avoid collisions. The normalized vortex force field is the attractive force field of the APM.

Anti-collision. The purpose of the anti-collision component is to avoid collisions among agents and between agents and obstacles. The anti-collision component is made up of the static repulsive potential of the search space boundaries and potential obstacles, as well as the dynamic repulsive potentials of the agents. Following [5], the repulsive force F_{rep} should approach infinity as the distance d between the agent and obstacle goes to zero. Additionally, a minimum distance d_{min} is introduced within which the repulsive force is always greater than the maximum attractive force. Due to normalization of the vortexed force field, the maximum attractive force is one. As agents should not be affected by far away objects, the repulsive force should be zero if the distance is larger than some maximum distance d_{max}. Finally, the

function should be continuously and monotonically differentiable. In the swarm GSL strategy, an adaption of the FIRAS function presented in [5] is employed that satisfies the mentioned conditions. To avoid collisions, a repulsive force F_{rep} is calculated for each agent as follows:

$$F_{rep} = \begin{cases} \left(\frac{d_{min}^2}{\frac{1}{d_{min}} - \frac{1}{d_{max}}} \right) \left(\frac{1}{d} - \frac{1}{d_{max}} \right) \frac{1}{d^2} & , \text{ if } d \leq d_{max} \\ 0 & , \text{ otherwise} \end{cases} \tag{2}$$

The selection of parameters d_{min} and d_{max} is subject to the positioning accuracy and the safe distance at which agents can navigate past each other. The anti-collision component sums up all individual repulsive forces of an agent on each other agent and obstacle into a resultant repulsive force. The resultant repulsive forces are also vortexized according to Equation (1). To achieve optimal navigation, it is essential that the APM and anti-collision forces share the same spin direction, which necessitates a reverse rotation for the repulsion forces generated by the enclosing walls. The same spin direction aids in preventing deadlocks during obstacle avoidance.

2.2 Agents

The agents are conceptualized as reactive particles comprised of a bout detector and a motion controller. The bout detector, inspired from [6], operates as follows: Agents calculate the second derivative of the measured concentration signal. Agents observe the second derivative to identify a positive zero crossing, termed as a bout. A bout signifies that a sensor has encountered a new plume filament. Since the sensor readings and therefore the bout detection is exposed to noise, noise-induced bouts are to be filtered out. First, the raw signal and both derivatives undergo smoothing through an exponentially weighted moving average (EWMA) filter. The EWMA filter is employed by the following function:

$$x_{s,i} = \alpha x_i + (1 - \alpha) x_{s,i-1}, \quad \text{with} \tag{3a}$$

$$\alpha = 1 - e^{-ln(2)/\tau}, \tag{3b}$$

where x_i denotes the raw value of the current iteration, $x_{s,i}$ and $x_{s,i-1}$ denote the smoothed value at the current and previous iterations respectively, and τ represents the half-life of the raw values in terms of the iteration count. Second, a threshold is introduced to discard bouts not exceeding the threshold. The positions of accepted bouts are transmitted to the artificial environment. The artificial environment integrates the bouts into the APM as pheromone markers.

The motion controller steers the agents and switches between two attraction modes. The first mode guides the agents to exploit the swarm knowledge by pursuing the attractive force emanating from the APM. In the second mode, agents follow the attractive force from a randomly generated setpoint for exploration of the search space. The attractive force of the random setpoint, denoted as $\vec{F}_{set}$, is calculated as:

$$\vec{F}_{set} = \begin{cases} \frac{\vec{X}_{set} - \vec{X}_{pos}}{\left\| \vec{X}_{set} - \vec{X}_{pos} \right\|} & , \text{ if } \left\| \vec{X}_{set} - \vec{X}_{pos} \right\| > \varepsilon \\ \frac{\vec{X}_{set} - \vec{X}_{pos}}{\varepsilon} & , \text{ otherwise} \end{cases} \tag{4}$$

where $\vec{X}_{pos}$ and $\vec{X}_{set}$ represent the position vectors of the agent and setpoint, respectively, and ε is the distance in which the agent linearly reduces speed. Subsequently, the force $\vec{F}_{set}$ is normalized. The motion controller will switch modes if the active attractive force, either towards the pheromone gradient or to the random setpoint, falls below some threshold force, indicating a lack of pheromone or reaching the vicinity of the random setpoint, respectively. Also, the motion controller switches modes after a maximum duration of the active mode. The calculated force is adjusted by the maximum linear velocity to obtain the velocity vector, which is passed to the low-level controller of the aerial robot.

3 Implementation and validation

In the first subsection 3.1, the aerial robot swarm and its components are described. In subsection 3.2, the implementation of a simulation is specified. In the simulation, the potential of bouts as a source proximity indicator is validated. In subsection 3.3, the swarm GSL strategy is validated in real-world experiments.

3.1 Aerial robot swarm

To validate the swarm GSL strategy, a swarm of palm-sized Crazyflie 2.0 quadrocopters (Bitcraze AB, [7]) is used. Each quadrocopter of the swarm is equipped with a 3D local positioning system [8] and a customized sensor deck that includes two SGP30 metal-oxide semiconductor gas sensors (Sensirion, [9]) and an optical motion detection system [10]. A quadcopter is shown in Figure 1.

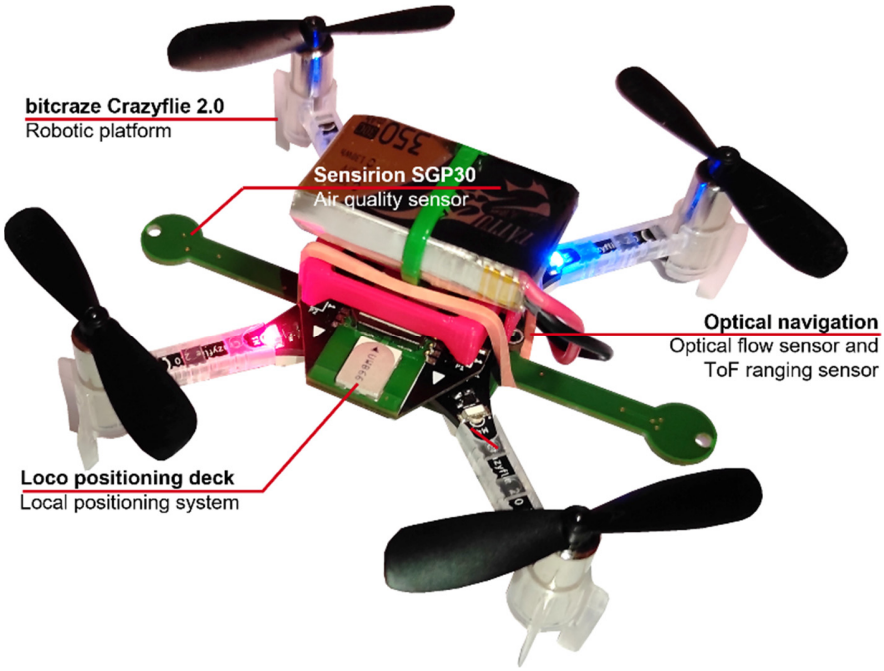

Fig. 1. The Crazyflie 2.0 quadrocopter platform with mounted sensors.

The 3D local positioning system estimates the absolute indoor 3D position of the copter. The aerial robot measures its distances to a set of distributed Ultra-wideband-based anchors based on continuously transmitted synchronization packets from these anchors. The distances are used to calculate the absolute position of the robot, which can be used for autonomous flight and collision avoidance. With the local positioning system, an accuracy of about 0.1 m is realized. The gas sensor consists of two pixels, one sensitive to hydrogen (H_2) and the other sensitive to ethanol (C_2H_5OH). From the readings of the two pixels, the sensor is able to calculate the total volatile organic compound and CO_2 equivalent onboard. As the real-world experiments, described in subsection 3.3, are performed with ethanol, only the transient signals of the ethanol pixel are used for detecting bouts. The ethanol pixel is specified for a range of 0.3 to 30 ppm, with an accuracy of 15% of the measured value. With the sensors and battery mounted on the quadrocopter, a take-off weight of ≈ 39.6 g and flight times of up to 5 minutes are achieved. The swarm GSL strategy proposed in this study is implemented using the Robot Operating System (ROS) and the Crazyswarm Python API [11].

3.2 Simulation

The potential of bouts to indicate the gas source proximity was validated through simulations using GADEN [12]. GADEN is a simulation framework developed in ROS, specifically designed for mobile robotic systems and gas sensing algorithms in the field of MRO. In the simulation, 12 agents were deployed in a rectangular room measuring (6×10) m^2. The room has two openings, one serving as the inlet and the other as the outlet. A single gas source was placed at coordinates (3.0, 1,5, 075) m. The simulation incorporated a pre-calculated wind field from GADEN, featuring strong, fluctuating airflow. The agents traversed the room by approaching random setpoints at 0.5 m height. A screenshot of the simulation of the visualization tool RViz in ROS is shown in Figure 2.

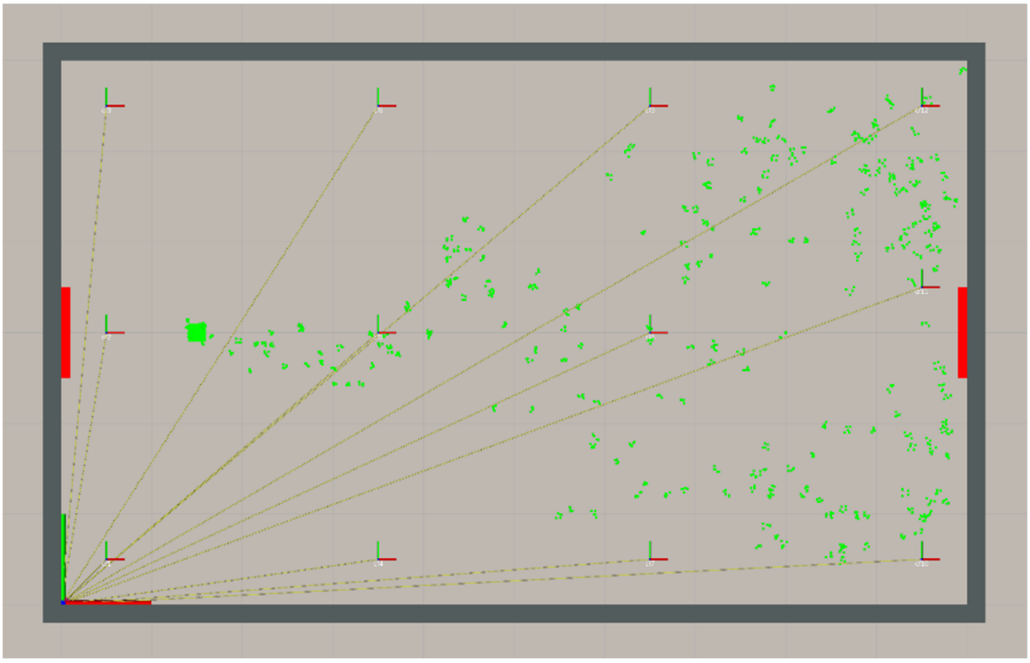

Fig. 2. Screenshot of the simulated environment in RViz, a visualization tool for ROS.

The agents logged the sensor measurements and positions at 10 Hz. The simulation, accelerated 10 times, ran for 30 minutes, resulting in approximately 180,000 sensor readings. Figure 3(a) illustrates mean sensor readings, where lower resistances correspond to higher concentrations. Figure 3(b) depicts the total bout count per cell. The figures visualize the readings in discrete maps of the search space. Both maps exhibit clusters of cells with low resistances and high bout counts near the source, although offset by 1.5 m in the airflow direction. While the gradients in Fig. 3(a) appear relatively smooth with no visible boundaries, the clusters in Fig. 3(b) display a denser V-shaped distribution including steep gradients in the downwind direction. The simulation results suggest that the bout count may serve as a more accurate and less noisy indicator of source proximity compared to the mean concentration.

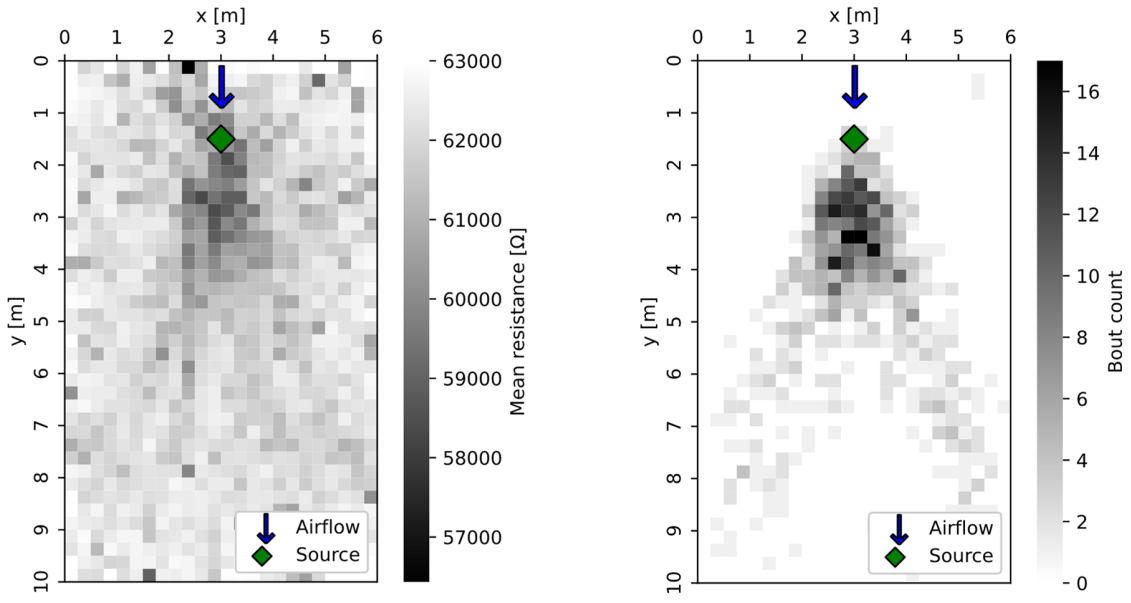

(a) Mean readings **(b)** Total bout counts

Fig. 3. Maps of the simulated sensor data.

3.3 Real-world experiments

The validation of the swarm GSL strategy is conducted through real-world experiments. A trio of aerial robots is deployed in a cuboid indoor environment, featuring a 2D search space of approximately (3×3) m² with a single gas source, as depicted in Fig. 4. The gas source, comprising a bottle of liquid ethanol connected to a tube and a 1 W fan, is positioned at (0.80, 0.75) m, elevated 0.1 m above the ground. To stimulate evaporation, pressurized air is introduced, and the emission rate is indirectly controlled by maintaining the airflow at 2 l/min. The source faces the center of the search space and opens roughly 1 minute before each run. Between runs, the source is closed, and the room is ventilated to ensure comparable starting conditions. Runs conclude either with the robots landing, crashing or running out of battery. Algorithm parameters were chosen heuristically. Sensor readings were logged at 10 Hz. Over 16 runs, around 20,000 measurements were recorded, with individual flight times ranging from 0 s (crash at takeoff) to 329 s. The combined flight times of all three quadrocopters range from 303 s to 903 s, with a mean of 613.4 s ± 165.2 s.

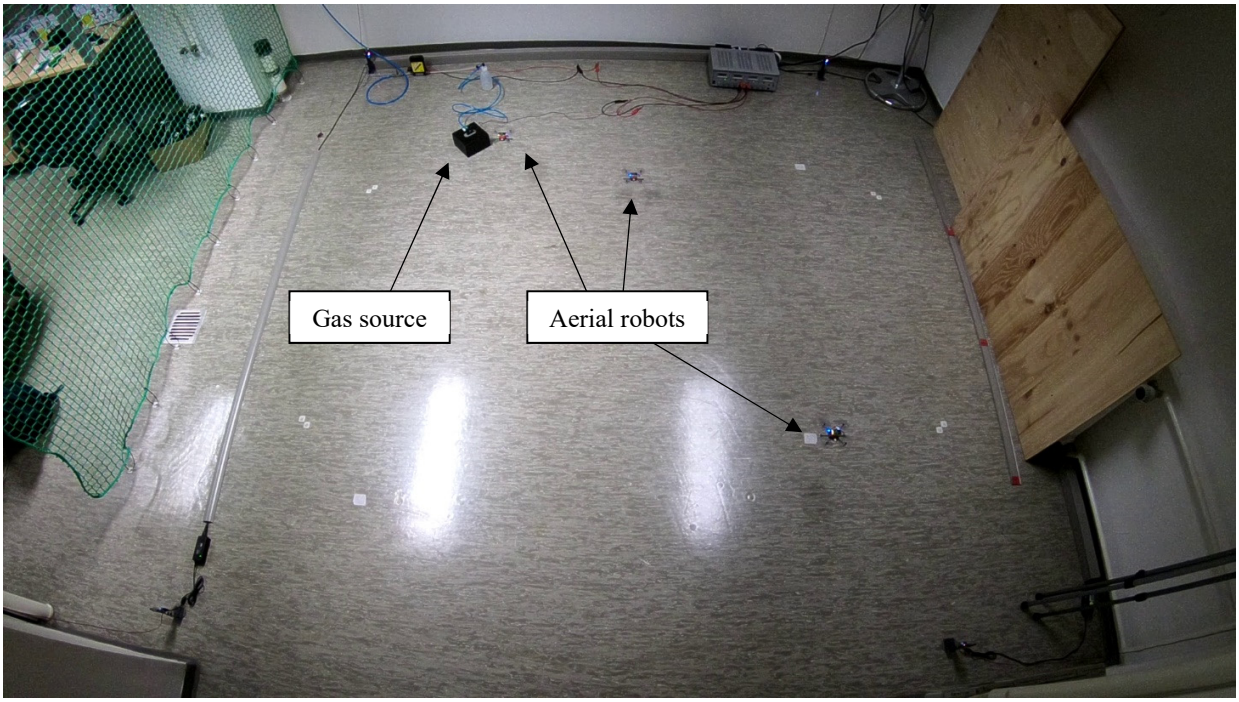

Fig. 4. Real-world experiments.

The experimental results are presented in Figs. 5 and 6. Fig. 5(a) displays a mean resistance plot with smooth gradients, akin to Fig. 3(a). However, in contrast to the simulation results, the cluster of low mean resistance is shifted in the upwind direction. In Fig. 5(b), bout distributions again showcase dense clusters with steep gradients, but unlike the simulation, no V-shape is evident. Fig. 6(a) illustrates the final source location estimates, with all estimation errors in the airflow direction. Notably, the mean error aligns closely with the center line of the airflow of the fan. Fig. 6(b) displays the average estimation error of the combined flight time scaled by the number of active agents, encompassing results from each individual run. The source estimation, on average, improves rapidly during the initial 90 s of combined flight time. After 330 s, the final source estimation error averages 0.7 m ± 0.29 m, ranging from 0.25 m (run #10) to 1.28 m (run #8). Improvement continues after 540 s, reducing the error to 0.6 m ± 0.21 m.

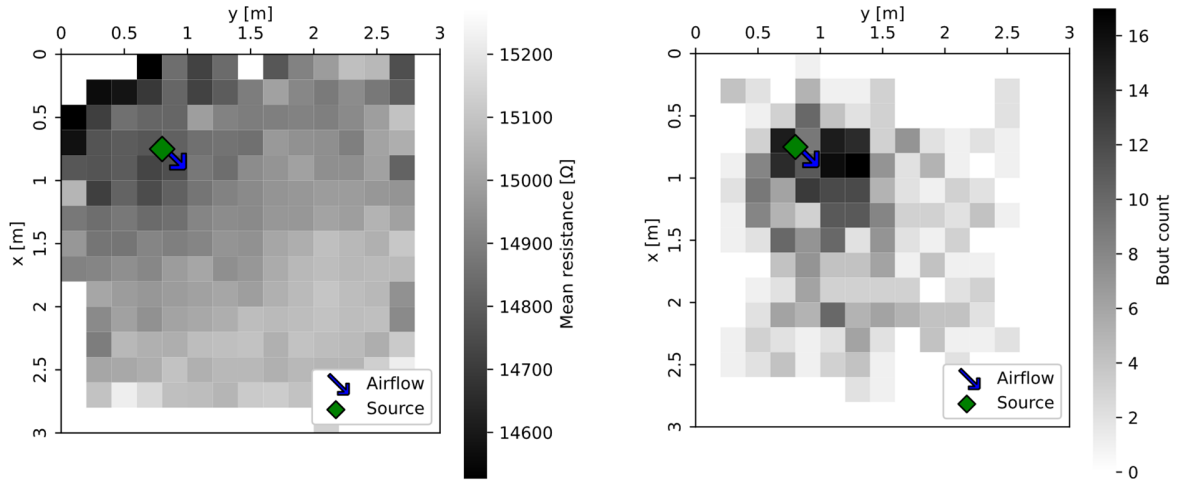

(a) Mean readings **(b)** Total bout counts

Fig. 5. Maps of the real-world sensor data.

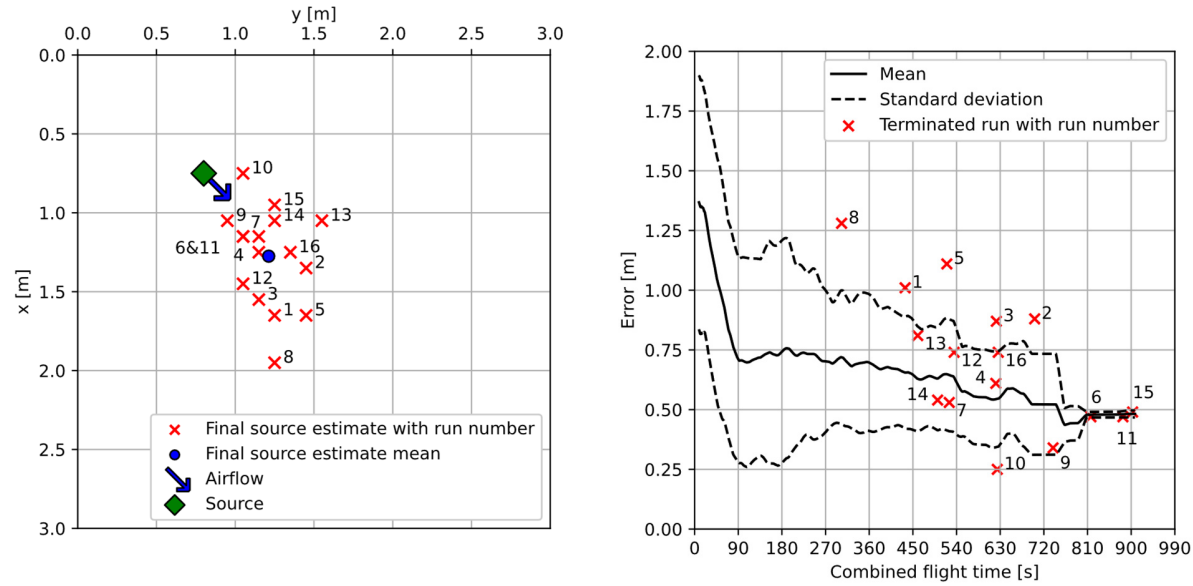

(a) **(b)**

Fig. 6. Experimental results: (a) Final estimations in space and (b) smoothed mean error of combined flight time of the experiments with standard deviation over time. Run time individually scaled by the number of active agents, and estimations excluded after termination.

4 Conclusions and future work

This paper has presented a swarm GSL strategy utilizing bouts as indicators of source proximity and virtual pheromone communication for swarm cooperation. Unlike previous studies conducted in this field, the swarm GSL strategy proposed herein is characterized by the integration, storage, and propagation of pheromone signals, rendering this study scalable, robust to noise and errors, responsive to changes in source position, and streamlining agents to a purely reactive nature. Both simulations and real-world experiments underscore the effectiveness of bouts as robust indicators in indoor environments, outperforming the use of mean concentrations. Despite being in its early stages, the proposed strategy exhibits promising outcomes in real-world experiments. Future research could concentrate on refining the parameter set of the swarm GSL strategy, which was chosen heuristically in this study. Enhancements might be attained by incorporating wind information and expanding the strategy into three dimensions. Additionally, a comparative analysis of the swarm GSL strategy against existing algorithms under identical environmental conditions could offer valuable insights.

References

1. Jing, T., Meng, Q.-H., & Ishida, H., 2021: Recent progress and trend of robot odor source localization. IEEJ Transactions on Electrical and Electronic Engineering 16(7), pp. 938-953.
2. Wang, J., Lin, Y., Liu, R., & Fu, J., 2021: Odor source localization of multi-robots with swarm intelligence algorithms: A review. Frontiers in Neurorobotics 16.
3. Schmuker, M., Bahr, V., & Huerta, R., 2016: Exploiting plume structure to decode gas source distance using metal-oxide gas sensors. Sensors and Actuators B: Chemical 235, pp. 636-646.
4. Meng, Q.-H., Yang, W.-X., Wang, Y., & Zeng, M., 2010: Multi-robot odorplume tracing in indoor natural airflow environments using an improved aco algorithm. In: Proceedings of the 2010 IEEE International Conference on Robotics and Biomimetics. Tianjin, China, December 14, 2010.
5. Khatib, O., 1985: Real-time obstacle avoidance for manipulators and mobile robots. In: Proceedings of the 1985 IEEE International Conference on Robotics and Automation. St. Louis, MO, USA, March 25, 1985.
6. Burgués, J., Hernández, V., Lilienthal, A. J., & Marco, S., 2019: Smelling nano aerial vehicle for gas source localization and mapping. Sensors 19(3), 478.
7. Bitcraze AB, 2023. Crazyflie 2.0. Accessed November 27, 2023, available at: https://www.bitcraze.io/products/old-products/crazyflie-2-0/.
8. Bitcraze AB, 2023. Loco Positioning system. Accessed November 27, 2023, available at: https://www.bitcraze.io/documentation/system/positioning/loco-positioning-system/.
9. Sensirion AG, 2020. Datasheet SGP30 – Sensirion Gas Platform. Accessed November 27, 2023, available at: https://sensirion.com/media/documents/984E0DD5/61644B8B/Sensirion Gas Sensors Datasheet SGP30.pdf.
10. Neumann, P. P., Hirschberger, P., Baurzhan, Z., Tiebe, C., Hofmann, M., Hüllmann, D., & Bartholmai, M.: Indoor air quality monitoring using flying nanobots: Design and experimental study. In: Proceedings of the 2019 IEEE International Symposium on Olfaction and Electronic Nose. Fukuoka, Japan, May 26, 2019.
11. Preiss, J. A., Honig, W., Sukhatme, G. S., & Ayanian, N.: Crazyswarm: A large nano-quadcopter swarm. In: Proceedings of the 2017 IEEE International Conference on Robotics and Automation. Singapore, Singapore. May 29, 2017.
12. Monroy, J., Hernandez-Bennets, V., Fan, H., Lilienthal, A. J., & Gonzalez-Jimenez, J., 2017: Gaden: A 3d gas dispersion simulator for mobile robot olfaction in realistic environments. Sensors 17(7), 1479.